AIP | Review of Scientific Instruments

Fast sweep-rate plastic Faraday force magnetometer with simultaneous sample temperature measurement

D. Slobinsky, R. A. Borzi, A. P. Mackenzie, and S. A. Grigera

Citation: Rev. Sci. Instrum. **83**, 125104 (2012); doi: 10.1063/1.4769049
View online: http://dx.doi.org/10.1063/1.4769049
View Table of Contents: http://rsi.aip.org/resource/1/RSINAK/v83/i12
Published by the AIP Publishing LLC.

Fast sweep-rate plastic Faraday force magnetometer with simultaneous sample temperature measurement

D. Slobinsky,[1] R. A. Borzi,[2] A. P. Mackenzie,[1] and S. A. Grigera[1,3]
[1]*SUPA, School of Physics and Astronomy, University of St Andrews, St Andrews KY16 9SS, United Kingdom*
[2]*Instituto de Investigaciones Fisicoquímicas Teóricas y Aplicadas (UNLP-CONICET) and Departamento de Física, UNLP, La Plata 1900, Argentina*
[3]*Instituto de Física de Líquidos y Sistemas Biológicos, UNLP-CONICET, La Plata 1900, Argentina*

(Received 4 September 2012; accepted 11 November 2012; published online 7 December 2012)

We present a design for a magnetometer capable of operating at temperatures down to 50 mK and magnetic fields up to 15 T with integrated sample temperature measurement. Our design is based on the concept of a Faraday force magnetometer with a load-sensing variable capacitor. A plastic body allows for fast sweep rates and sample temperature measurement, and the possibility of regulating the initial capacitance simplifies the initial bridge balancing. Under moderate gradient fields of ∼1 T/m our prototype performed with a resolution better than 1×10^{-5} emu. The magnetometer can be operated either in a dc mode, or in an oscillatory mode which allows the determination of the magnetic susceptibility. We present measurements on $Dy_2Ti_2O_7$ and $Sr_3Ru_2O_7$ as an example of its performance. © *2012 American Institute of Physics*. [http://dx.doi.org/10.1063/1.4769049]

I. INTRODUCTION

The magnetisation (**M**) of a macroscopic body can provide information on the microscopic magnetic degrees of freedom and their dynamics. The relevance of **M** goes beyond the study of systems at equilibrium: particularly in spin glasses, but in any material where the characteristic time of the magnetisation measurement is similar to the relaxation time of the spin system, *time* is a key additional parameter. While the spin relaxation time becomes longer at low temperature, the dynamics of a magnetic system can be explored by measuring, at fixed temperature, the magnetisation as a function of **B** for different field sweep rates. For measurements like these, it is particularly important to develop instrumentation that allows measurement at fast sweep rates. Rapid sweep apparatus also has many other applications and advantages, for example in single-shot low temperature measurements.

Rapid sweeping can be particularly problematic in the sub-Kelvin regime, where the available cooling power can be very low. In this paper we report on the design and performance of a plastic Faraday-type magnetometer which minimises the effects of low cooling power. The choice of material allows for relatively fast sweep rates (≈0.2 T/min) with minimum heat dissipation. We have tested the operation in the sub-Kelvin high field regime both in static and in oscillating gradient field, the latter giving both the magnetisation and the susceptibility of the sample. The organisation of the paper is as follows. In Sec. II, we summarize the methods generally used to measure the magnetic moment of a sample. In Sec. III, we present the main design features of our probe design. The performance is discussed in Sec. IV, where we present the results obtained in two different materials: the spin-ice material $Dy_2Ti_2O_7$, an insulating frustrated magnet, and the a strongly correlated metal $Sr_3Ru_2O_7$, which shows metamagnetism at high fields.

II. MAGNETOMETRY

Basic methods to measure bulk magnetisation can be separated into two main categories.

A. Inductively coupled methods

In this case the sample sits inside a coil and the magnetic induction is measured by either modulating the magnetic field (where the magnetic response rather than **M** is measured) or moving the sample and coil relative to each other in an oscillatory fashion (vibratingsample magnetometry/vibrating coil magnetometry).[1,2] Although both these alternatives have been successfully applied over large temperature regimes, they are less suitable for sub-Kelvin temperatures where heating due to eddy currents or the mechanical movement of the magnetometer can affect the measurement. These problems are usually overcome at the expense of using dilution refrigerators with large cooling power and/or with the loss of simplicity of the probes. Other possibilities include the use of superconducting quantum interference devices for the readout. This, although suitable for low temperatures, is relatively slow and difficult to implement for high magnetic fields.

B. Force methods

Here the magnetisation is determined by measuring the force a magnetic sample experiences in an inhomogeneous magnetic field, typically using a Faraday balance. The magnetisation is extracted from the equation

$$\mathbf{F} = \mu \cdot \nabla \mathbf{B}, \tag{1}$$

where $\nabla \mathbf{B}$ is assumed to be homogeneous within the sample,[3] and μ is the total magnetic moment of the sample.

The optimum type of Faraday force magnetometry varies according to the experimental circumstances. In the high

temperature range the most commonly used configuration has been a balance with an arm compensated at room temperature, and the other arm in the cryogenic environment. Capacitive balances have been implemented for the sub-Kelvin regime,[4,5] with the advantage that the whole experimental setup resides within the cryogenic environment, avoiding the heat leak implied by balancing at room temperature. **M** is sensed by the change of the capacitance between two parallel plates, one fixed, and the other movable. The force exerted by a sample attached to the movable plate, Eq. (1), is compensated by the restoring force of a spring. The use of this type of design is simple and practical in the range of temperatures where the spring constant generating the restoring force is essentially temperature independent. The main drawback of any force methods is the difficulty of avoiding spurious changes in the capacitance due to the action of torques that arise from either intrinsic magnetic anisotropy or from the geometry of the sample.

One of the advantages of the Faraday method is that the magnetisation measurement can be integrated with other measurements,[6] using the balance as a platform. In our case, we have developed a simple Faraday force magnetometer for the specific purpose of measuring the magnetisation and the instantaneous temperature of the sample, which has proved to be useful when investigating dynamical magnetisation processes.

III. DESIGN OF THE MAGNETOMETER

The magnetometer was designed to fit into the 35 mm vacuum can of a dilution refrigerator with a nominal cooling power of 25 μW at 100 mK (Kelvinox 25, Oxford Instruments). The main magnet (Oxford Instruments) generates a magnetic field of up to 15 T, while two superconducting modulation coils in a Helmholtz gradient configuration can produce field gradients of less than 1 T/m. A sketch of the magnetic system and the capacitive magnetometer is shown in Figure 1. Although we have not tested it in a higher static field than 15 T there is no reason in principle for it not to work well in much higher fields.

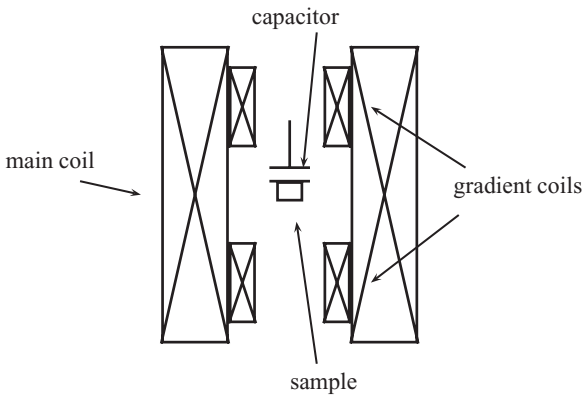

FIG. 1. Schematic view of the magnetic system and load cell. The capacitively sensed load cell is in the homogeneous magnetic field of a 15 T main coil and in the centre of a set of Helmholtz coils in gradient configuration.

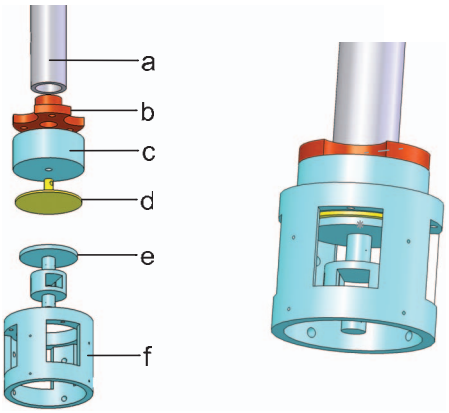

FIG. 2. (Right) Plastic magnetometer. (Left) The two assemblies that form the magnetometer: the rod assembly includes (a) hollow stainless steel rod from the mixing chamber to the center of the magnet, (b) oxygen free copper adapter, (c) threaded Tufset piece, and (d) top plate of the capacitor made of brass. The magnetometer assembly is entirely made of Tufset and includes (e) sample holder + movable capacitive plate and (f) body.

We chose to build the magnetometer out of plastic (Tufset–Tufnol Composites Limited) with the main purpose of avoiding eddy current heating during the magnetic field sweeps. For maximum simplicity, it consists of two assemblies, each of them containing one plate of the sensor capacitor. The first one (pieces (a)–(d) in Figure 2), which hosts the fixed capacitance plate, includes the rod (piece (a)) leading from the mixing chamber of the dilution refrigerator to the centre of the magnet. The second one includes the magnetometer assembly containing two pieces: a body (piece (f)) that screws into the first assembly, and a sample holder (which includes the movable capacitor plate) suspended by wires (piece (e)). For this small design we inverted the geometry from Ref. 5 by placing the movable capacitor plate above the sample holder as depicted in Figure 2. In this way, the magnetometer assembly screws into the probe rod, allowing control over the initial capacitance.

The magnetometer body consists of a hollow cylinder of 20 mm outer and 18 mm inner diameter, machined out of a single piece of Tufset. Four windows were made to allow easy access to the sample holder that sits in its centre.

The sample holder is also machined out of a single piece of Tufset. We painted the capacitor plate on it (Figure 3) with room temperature air-cured silver paste (4929N, DuPont) and then linked it to a connector on the magnetometer body with a 25 μm diameter gold wire. The sample space on this piece is 4 mm by 3 mm and 8 mm in depth. This space is divided into two by a sapphire plate of thickness 0.2 mm that slides into a perpendicular slot and is fixed with vacuum grease (Apiezon N), leaving effectively a sample space of 4 mm in depth (left of Figure 3). The sapphire acts as an orientation plane for the sample that is attached to it with vacuum grease as shown in the central part of Figure 3.

The sample holder is fixed in position with nylon fishing line of diameter 0.19 mm that is threaded through holes (two on the top part of the rod and two on the bottom part of it, see Fig. 3) drilled in it, and through eight cone-shaped holes drilled in the spaces between the windows of the body. Once

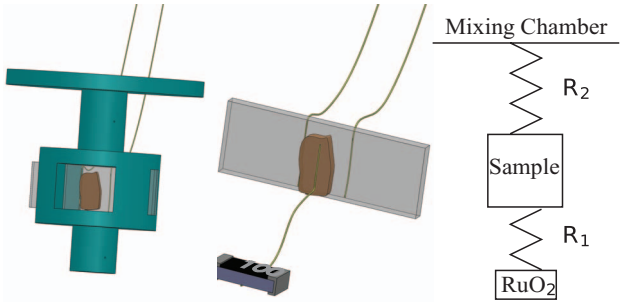

FIG. 3. (Left) Sample holder with sapphire plate and sample. (Centre) Detail of the sapphire plate. Gold wires at the back of it are used to thermalise the sample that is greased to the front of the plate. The sample is connected by another gold wire to a RuO_2 thermometer hanging from the magnetometer body by its contacts. (Right) Thermal resistance diagram, R_1 is much lower than R_2.

threaded, the lines are glued in position with epoxy (#1266, Stycast). These lines provide the restoring force for the moving plate of the capacitor, and the choice of material and geometry is vital to define the sensitivity of the magnetometer.

Given the constraints in our case, we chose to design a small magnetometer that would not need the use of a centering mechanism. This reduces the theoretical sensitivity, which for a simple model of the deflection of a beam is proportional to L^3, with L the length of the wires from the inner diameter to the sample holder at the centre.[7] We partially compensated this by the choice of nylon fishing line, which in addition of being non-metallic, has a low elastic constant.

Thermal anchoring of the sample is achieved through two 25 μm gold wires of negligible spring constant. These wires link a connector on the magnetometer body with the back of the sapphire plate, where they are bonded with silver paste (6838, Dupont). Finally, a thick 0.5 mm silver wire thermally grounds the connector to the mixing chamber. In this way, the sapphire plate is the main thermal link between the sample and the mixing chamber.

In order to measure the temperature of the sample, we attached with silver paste a 25 μm gold wire from the sample to the back of a bare 1 kΩ RuO_2 chip (crg0805 smt, Tyco Electronics). In this way we obtained a much lower thermal resistance between the sample and the thermometer, R_1, than between the sample and the mixing chamber R_2 (see Fig. 3).

For efficient setup of the experiment, it is desirable to tune the initial capacitance at room temperature. This is achieved by screwing the body assembly into the rod assembly. To avoid twisting wires during this process, there are connectors on the magnetometer body assembly for all wires coming from the stainless steel rod, namely the manganin thermometer wires, the miniature co-axial cable (type SS, Lakeshore) and the thermal link to the mixing chamber.

IV. EXPERIMENTAL RESULTS

We tested the performance of our magnetometer on two systems with very different characteristics: one is the frustrated magnet $Dy_2Ti_2O_7$, an insulator with large magnetic moments which shows strong out of equilibrium magnetisation jumps below 650 mK in low magnetic fields (below 1 T).[9] Here, the simultaneous measurement of the sample temperature is invaluable for understanding the non equilibrium processes. The other system is $Sr_3Ru_2O_7$, a strongly correlated paramagnetic metal with a series of metamagnetic jumps of approximately 0.1 μ_B/Ru between 7.5 and 8.5 T,[14] on which we could test the performance of the magnetometer up to magnetic fields of 15 T.

A. Magnetisation and temperature measurements on $Dy_2Ti_2O_7$

We tested the low magnetic field performance of our magnetometer on the frustrated magnet $Dy_2Ti_2O_7$, a cooperative paramagnet of the spin-ice family.[8] The magnetic moments come from Dy ions residing on the vertices of a pyrochlore lattice; because of strong single ion anisotropy, the ground state of the Dy^{3+} can be thought as an Ising doublet with local quantisation axis along the ⟨111⟩ crystallographic axis. The combination of lattice geometry, exchange and a dipolar interaction arising from the very large Dy magnetic moments (approximately 10μ_B) results in a frustrated ground state with a degeneracy growing exponentially with the size of the system. A freezing transition occurs at about 650 mK, below which the system develops out-of-equilibrium dynamics for any experimentally achievable time. A detailed study of the phenomena can be found in Ref. 9.

A single crystal of $Dy_2Ti_2O_7$ was grown by the floating zone method in St Andrews University, Laue oriented and cut into a prism of $\sim 2 \times 0.7 \times 0.5$ mm^3 with the long axis along [111]. The sample was mounted on the sapphire plate as explained in Figure 3, with [111] parallel to both the magnetic field and its gradient. The free load capacitance (no applied gradient) in this experiment was 7.2 pF. The magnetic field and temperature were controlled from a PC which also records the capacitance measured with an automatic capacitance bridge operating at 1 kHz (2500 A, Andeen–Hagerling). This bridge and a resistance bridge (SIM 921AC, Stanford Research Systems) which measures the RuO_2 thermometer on the sample were set to give a data point per second. External vibrations were damped by placing the cryostat dewar on the platform of an active vibration-isolation system (vario 45/60/90, Halcyonics). The main magnet field was swept at constant rate while the gradient coils are fixed with a constant value of $\sim$1 T/m. The measurements were calibrated by comparing the magnetisation vs. field curves at 4 K with those taken in a squid magnetometer (quantum design MPMS).

Figure 4(a) shows the raw data for the low field part of the magnetisation curve at base temperature ($\sim$80 mK) for different sweep rates. The resolution on these curves is better than 1×10^{-5} emu. The out-of-equilibrium behaviour of this cooperative paramagnet can be inferred from the dependence of the magnetisation on the sweep rate. For slow sweep rates **M** follows a smooth curve which becomes increasingly undulating as the sweep rate is increased, until it eventually becomes discontinuous with a very sharp jump of about 50% of the saturation value (of 5μ_B/Dy for this orientation[10]). Panel (b) of this figure shows the simultaneous temperature reading from the calibrated RuO_2 thermometer connected to the sample.

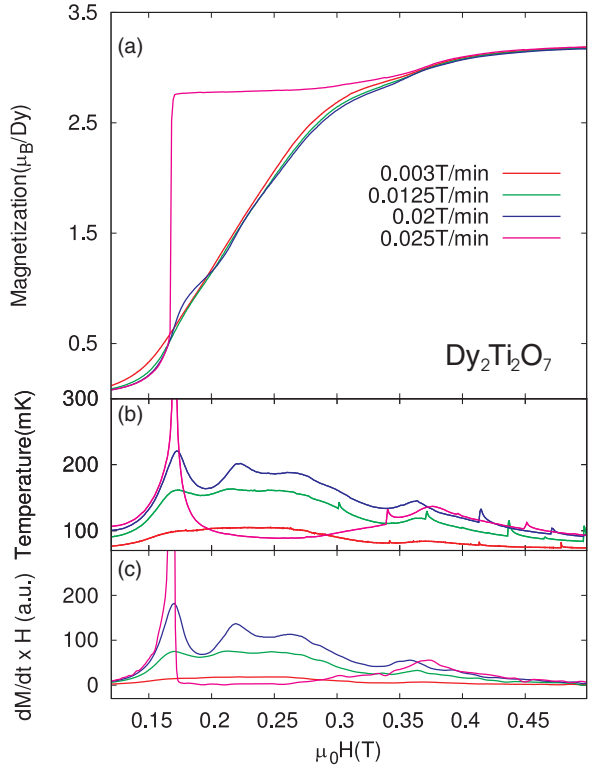

FIG. 4. (a) Magnetisation vs. magnetic field of $Dy_2Ti_2O_7$ for different sweep rates measured with the cryostat at base temperature ($T_{mch} \sim 80$ mK). (b) Sample temperature vs. magnetic field, as measured from the RuO_2 thermometer simultaneously with the magnetisation shown in (a). The small spikes above 0.3 T are spurious effects due to spikes in the external magnetic field (caused by flux jumps in the main coil of our magnet) resulting in small temperature changes. (c) Derivative of the magnetisation with respect to time multiplied by the magnetic field (i.e., rate of heat generation) as a function of magnetic field.

Our capability of measuring temperature allows a simple thermal analysis that gives insight into the underlying physics. The sample is strongly thermally coupled to the mixing chamber; so changes in the sample temperature are proportional to the power being dissipated in the magnetisation process (see below). This can be seen comparing the temperature in panel (b) with panel (c), where the heat produced in the process per unit volume and unit time, $\mu_0\mathbf{H} \cdot \frac{d\mathbf{M}}{d(\mu_0 H)} \times$ field sweep rate, is plotted as obtained from the data in panel (a).

To analyse the temperature data more rigorously one can do a simple thermal modelling of the system. The production and diffusion of heat from the sample to the mixing chamber is ruled by the continuity equation: $\frac{du}{dt} + \nabla \cdot \mathbf{J} = w(t, \mathbf{r})$, were u is the internal energy of the crystal per unit volume, $\mathbf{J}$ is the heat density current, and $w(t, \mathbf{r})$ is the heat delivered locally to the lattice per unit volume and unit time. Due to the way we designed the probe and thermally anchored the sample, it is reasonable to assume that the delivered magnetic energy either remains within the sample, raising its temperature $T(t)$, or flows towards the mixing chamber of the cryostat, building up a total heat current $I_{th}(t)$. Integrating the continuity equation over the volume of the sample, and using Fourier's law to express I_{th}, we can write

$$C_p \frac{dT}{dt} = 1/R_{th}(T(t) - T_{\mathrm{mch}}) + V\mu_0\mathbf{H} \cdot \frac{d\mathbf{M}}{dt}, \qquad (2)$$

where $T(t) - T_{\mathrm{mch}}$ is the difference between the temperature of the sample (directly measured by our thermometer) and that of the mixing chamber; R_{th} is the thermal resistance of the link between these two points, C_p the specific heat of the sample, and V its volume.

The specific heat of $Dy_2Ti_2O_7$ is very small in the region of parameters of Figure 4 (see Ref. 11), implying a very short relaxation time (in the scale of our measurements). This means that the left hand side of (2) can be neglected with respect to any of the terms in the right, which tend to balance each other. The sample is then in a quasi-stationary state ($C_p \frac{dT}{dt} \approx 0$) at all times, giving the proportionality measured between Figs. 4(b) and 4(c): $T = T_{mch} + R_{th}\mu_0\mathbf{H} \cdot \frac{d\mathbf{M}}{dt}$. In practice, it was then possible to identify the microscopic process as a release of Zeeman energy during the out-of-equilibrium processes.

B. Magnetisation measurement on $Sr_3Ru_2O_7$

The ruthenate $Sr_3Ru_2O_7$ was used to test the performance of the probe at high fields and to test the method of gradient field modulation to measure susceptibility. At low temperatures, $Sr_3Ru_2O_7$ is a paramagnetic Fermi liquid that undergoes a set of meta-magnetic first order transitions as a function of magnetic field. These transitions occur below ~1.2 K and in the neighbourhood of 8 T for field aligned close to the crystallographic c-axis. This material also provides a valuable test for the mechanical stability of the magnetometer given that for slight misalignments from the c-axis the magnetisation as a function of field lacks a feature around 12 T that is seen in torque measurements.[12]

We used the same experimental setup than in the case of $Dy_2Ti_2O_7$ and measured a single crystal of $Sr_3Ru_2O_7$ of dimensions $2.4 \times 2.5 \times 1.2\,\mathrm{mm}^3$. The free-load capacitance was of 26 pF, and the sample sat between 5° and 10° off the c-axis, as inferred from the known dependence of H_c with angle[13,14]). The raw signal was approximately quadratic in nature and of even parity with respect to the applied magnetic field. Given that the system is a well known paramagnet, this is contrary to the naive expectation of an odd signal as a function of applied magnetic field. This change in field parity is the consequence of a large torque component. To isolate each contribution we measured sets of data both with positive and negative field gradient: the magnetisation was extracted as the semi-sum of these data, while torque was the semi-difference. The torque and magnetisation signals are shown in Figure 5. Notice that, in accordance with Ref. 12, there is a very noticeable feature in the torque signal at about 12 T which is almost completely absent from the magnetisation curve. In another experiment with an initial capacitance of about 2.6 pF the raw data still showed a quadratic shape but with a much less pronounced behaviour.[15] Independent of the setup conditions, the subtraction and addition of the signals with positive and negative gradient fields has proven to give the right magnetisation and torque in all cases. However, the subtraction and addition reduce the sensitivity by up to an order of magnitude.

Using the same sample of $Sr_3Ru_2O_7$ we tested the idea suggested in Ref. 5 of alternating the gradient field to measure

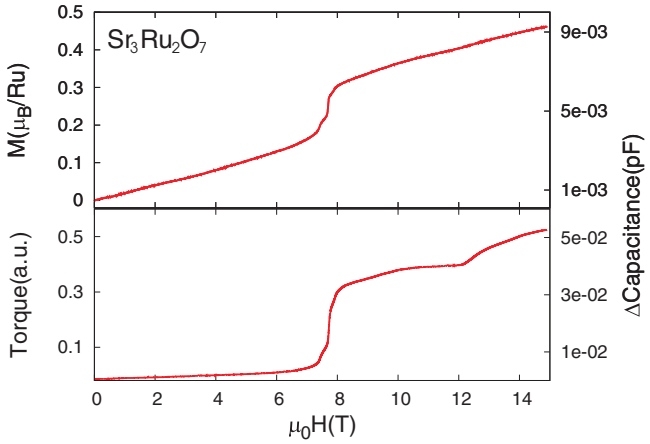

FIG. 5. (Top) The magnetisation of $Sr_3Ru_2O_7$, antisymmetric part of the raw signal with respect to the magnetic field gradient, extracted from the difference of sweeps with positive and with negative field gradient. (Bottom) Symmetric part, giving the torque. The right-hand side axis is proportional to the raw signal. Note that torque signal is almost an order of magnitude bigger than that for the magnetisation for this starting capacitance of 26 pF.

susceptibility. For this, we replaced the automatic capacitance bridge by a manual capacitance bridge (1616, General Radio) to which we connected two lock-in amplifiers (LIA) in series (SR830, Stanford Research Systems). The capacitor was excited with a frequency of 1 kHz and the signal measured with the first LIA. The second LIA drove the gradient coils at a low excitation frequency ν_D through a commercial hi-fi amplifier. The analogue channel output signal of the first LIA was fed as the input of the second LIA from where the signals at ν_D in the first and second harmonics were detected.

Figure 6 shows the real part of the susceptibility measured at $\nu_D = 3$ Hz around the meta-magnetic transitions. These data have signal-to-noise ratio comparable to previously reported field modulated susceptibility data,[14] where low-temperature transformers had been used to boost the signal. This technique is most useful to measure susceptibility when the frequencies are too low to give a good inductance signal, and is in principle limited in frequency by the mass of the sample stage. The range of frequencies could, in principle, be extended by employing feedback to measure while keeping the capacitor plates static.

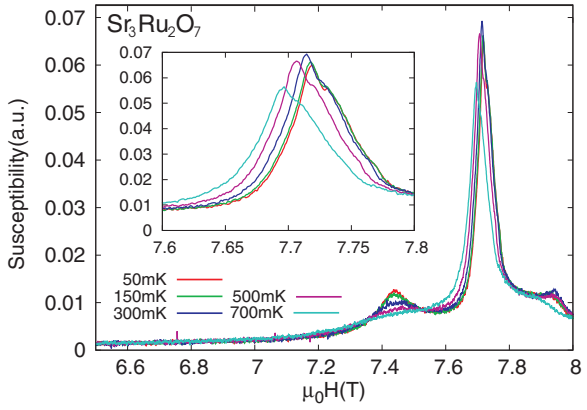

FIG. 6. Gradient modulation susceptibility at 3 Hz for different temperatures around the meta-magnetic transitions of $Sr_3Ru_2O_7$. Three main peaks can be seen with a noise comparable to the one on Ref. 14. Inset: blow up of the main peak.

V. CONCLUSIONS

We presented a newly designed plastic magnetometer with a resolution better than 10^{-5} emu capable of operating at millikelvin temperatures and under magnetic fields up to 15 T. The magnetometer was successfully integrated with a sample thermometer that measures the instantaneous change in temperature of the sample with high accuracy down to temperatures of approximately 50 mK. We demonstrated the possibility of extracting the torque signal from the raw signal and confirmed that the latter grows with the initial equilibrium capacitance. Furthermore, we showed that the same probe can be used to measure the magnetic susceptibility by modulating the gradient field at low frequencies, for which the usual inductive methods yield a very low signal.

ACKNOWLEDGMENTS

We wish to thank to E. A. Yelland, J. A. N. Bruin, and A. W. Rost for helpful discussions and for their help in the lab, and R. S. Perry and A. S. Gibbs for providing the crystals for the experiments. This work was done with the financial support of EPSRC and the Royal Society (UK) and CONICET (Argentina). A.P.M. acknowledges the receipt of a Royal Society Wolfson Research Merit Award.

[1] S. Foner, Rev. Sci. Instrum. **30**, 548 (1959).
[2] S. Legl, C. Pfleiderer, and K. Krämer, Rev. Sci. Instrum. **81**, 043911 (2010).
[3] Strictly, $\mathbf{F} = \nabla(\mu \cdot \mathbf{B})$.
[4] A. G. Swanson, Y. P. Ma, J. S. Brooks, R. M. Markiewicz, and N. Miura, Rev. Sci. Instrum. **61**, 848 (1990).
[5] T. Sakakibara, H. Mitamura, T. Tayama, and H. Amitsuka, Jpn. J. Appl. Phys. **33**, 5067 (1994).
[6] J. S. Brooks, M. J. Naughton, Y. P. Ma, P. M. Chaikin, and R. V. Chamberlin, Rev. Sci. Instrum. **58**, 117 (1987).
[7] See for example, L. D. Landau and E. M. Lifshitz, *Theory of Elasticity*, 2nd ed., Course of Theoretical Physics (Pergamon, 1981).
[8] For a review on spin-ice see S. T. Bramwell and M. J. P. Gingras, Science **294**, 1495 (2001).
[9] D. Slobinsky, C. Castelnovo, R. A. Borzi, A. S. Gibbs, A. P. Mackenzie, R. Moessner, and S. A. Grigera, Phys. Rev. Lett. **105**, 267205 (2010).
[10] T. Sakakibara, T. Tayama, Z. Hiroi, K. Matsuhira, and S. Takagi, Phys. Rev. Lett. **90**, 207205 (2003).
[11] R. Higashinaka, H. Fukazawa, K. Deguchi, and Y. Maeno, J. Phys. Soc. Jpn. **73**, 2845 (2004).
[12] E. Ohmichi, Y. Yoshida, S. I. Ikeda, N. V. Mushunikov, T. Goto, and T. Osada, Phys. Rev. B **67** 024432 (2003).
[13] S. A. Grigera, R. A. Borzi, A. P. Mackenzie, S. R. Julian, R. S. Perry, and Y. Maeno, Phys. Rev. B **67**, 214427 (2003).
[14] S. A. Grigera, P. Gegenwart, R. A. Borzi, F. Weickert, A. J. Schofield, R. S. Perry, T. Tayama, T. Sakakibara, Y. Maeno, A. G. Green, and A. P. Mackenzie, Science **306**, 1154 (2004).
[15] Higher initial capacitances amplified torque signals quadratically with inverse initial equilibrium distance.